Control Method to Suppress Stick-slip in Drill-strings Featuring Actuation Delay and Constraints

James MacLean [*], **Vahid Vaziri** [*], **Marian Wiercigroch** [*]
Sumeet S. Aphale [*]

[*] *Centre for Applied Dynamics Research, School of Engineering, University of Aberdeen, King's College, Aberdeen AB24 3FX*

Abstract: In this work, performance of a modified-integral resonant controller with integral tracking is investigated numerically under the effects of actuator delay and actuation constraints. Actuation delay and constraints naturally limit controller performance, so much so that it can cause instabilities. A 2-DOF drill-string with a nonlinear bit-rock interaction model is analysed. The aforementioned control scheme is implemented on this system and analysed under the effects of actuation delay and constraints and it is found to be highly effective at coping with these limitations. Lastly, the scheme is analysed in detail by varying its gains as well as varying system parameters, most notably that of actuation delay.

Keywords: Output feedback control; Control of constrained systems; Delay systems; Tracking; Parameter-varying systems

1. INTRODUCTION

In the Oil and Gas industry, drill-strings are critical engineering systems and structures for exploration and production drilling. Due to the complex dynamics inherent within drill-strings and their frictional interactions with the borehole, they are highly susceptible to unwanted oscillatory effects, of which the focus in this paper will be that of torsional (Real et al., 2018; Hohl et al., 2016; Jardine et al., 1994). More specifically, within the umbrella of torsional vibrations, the issue of Stick-Slip is considered (Kovalyshen, 2015). Stick-Slip is one of the most commonly encountered vibration phenomenon in any type of well and is the most common reason for down-hole tool and tool joint failure. Thus, Stick-Slip has garnered great interest in its cause as well as its necessary prevention. Stick-Slip studies began with the majority of its studies focusing on simplifying and isolating the Stick-Slip phenomenon to low DOF drill-string models (Navarro-López and Cortés, 2007; Navarro-López, 2009) based on the torsional pendulum. The friction model developed for lumped-mass modelling, is a discontinuous switch case one by Navarro-Lopez (Navarro-López and Cortés, 2007). In this paper, a 2-DOF vertical drill-string model is adopted and derived from first principles as the system of choice. The choice to use a 2-DOF model allows for a sufficiently complex system that demonstrates multiple rich dynamics of stick (no drilling), Stick-Slip and constant drilling to exist for a range of WOB and top torque values and is still relevant in the benchmarking of novel control schemes.

A number of strategies aimed at mitigating Stick-Slip oscillations have been reported in literature. In recent times, the μ-synthesis control method (Vromen et al., 2015, 2019) has been proposed as a way with which to overcome Stick-Slip oscillations, however this methodology relies on linearisation methods which only possess expected performance in a very small range around the equilibria of interest. There has also been the suggestion that a linear quadratic regulator based controller to suppress Stick-Slip using a discretised model of axial and torsional dynamics (Sarker et al., 2012). Another source suggested using WOB as a control parameter (Canudas-de Wit et al., 2008), but this requires knowing the exact WOB being applied at any given instant to a drill-string, which is a very challenging precondition. Consequently, this method lacks robustness in the face of uncertain values of WOB. PID and PD control has been proposed by (Bisoffi et al., 2020; Ritto and Ghandchi-Tehrani, 2019; Navarro-López and Suárez, 2004; Pavone and Desplans, 1994) as a way with which to avoid Stick-Slip. Soft-Torque control (patened by Shell in (Runia et al., 2013)) and Z-torque control (Kyllingstad, 2017) are effectively PI controllers and have great sensitivity to actuator delays and measurement delays which also belong to the PID family. None of these control methods are particularly robust to system parameters or bit-rock changes. In order to mitigate the very real problem of system parameter changes while making sure constant drilling occurs, Sliding-mode Control (SMC) has been thoroughly investigated (Vaziri et al., 2018; Navarro-López, 2009).

Drill-strings are subject to three main types of delay, namely; regenerative state-based cutting delay terms due to PDC heads, actuation delays and measurements delays. Actuation delays even exist in experimental setups such as the in-house experiment (Vaziri et al., 2018). There is a lack of detailed work with actuation delay. Some work in recent times has factored in studying the effects of state-based delay on PID performance on a lumped-mass model (Liu et al., 2014). In addition to Stick-Slip and actuation delay, there is also a lack of literature on actuation constraints affecting the ability to reach a de-

sired control outcome. In this paper, a combined control approach to tackling Stick-Slip featuring both actuation delay and constraints is considered by utilising the 'Modified Integral Resonant Control' (MIRC) with Integral Tracking (MacLean and Aphale, 2020). This combined control scheme is a simple, combination of two first-order controllers that work by adding two extra state equations to the system in question. It then includes the use of integral tracking to meet the desired criterion of constant drilling.
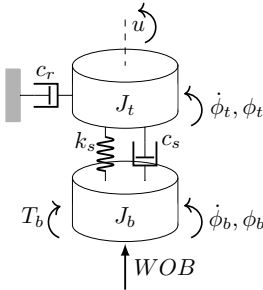
2. OPEN LOOP MODELLING

Fig. 1. Equivalent mechanical model for the experimental setup consisting of two rotational pendular interlinked with a rotational spring and damper. The model features a top-torque u with damping term c_r and nonlinear torque on bit friction model T_b.

In this section the open-loop model used, along with system parameters, is taken from Vaziri et al. (2018). The following differential equations represent what is shown in Fig.2;

$$J_t\ddot{\phi}_t + (c_s + c_r)\dot{\phi}_t + k_s\phi_t - c_s\dot{\phi}_b - k_s\phi_b = u, \quad (1)$$

$$J_b\ddot{\phi}_b + c_s\dot{\phi}_b + k_s\phi_b - c_s\dot{\phi}_t - k_s\phi_t = -T_b. \quad (2)$$

The friction model for T_b is defined in Navarro-López and Cortés (2007) and is a discontinuous switch model shown as follows:

$$T_b = \begin{cases} \tau_r, & \text{if } \|\dot{\phi}_b\| < \zeta \text{ and } \|\tau_r\| \le \tau_s \\ \tau_s \, \text{sgn}\,(\tau_r), & \text{if } \|\dot{\phi}_b\| < \zeta \text{ and } \|\tau_r\| > \tau_s \\ \mu_b R_b WOB \, \text{sgn}\left(\dot{\phi}_b\right), & \text{if } \|\dot{\phi}_b\| \ge \zeta. \end{cases} \quad (3)$$

The adopted friction model operates the drill-string in one of the three key phases. Phase 1 is the sticking phase in which the bit is not moving ($\dot{\phi}_b < \zeta$) due to the static friction torque τ_s being equal to or more than the absolute value of the reaction torque τ_r: $\|\tau_r\| \le \tau_s$. Phase 2 is the stick-to-slip shase in which the bit just about to move ($\dot{\phi}_b < \zeta$) as the static friction torque τ_s is less than the absolute value of the reaction torque τ_r: $\|\tau_r\| > \tau_s$. Phase 3 is the slip phase in which the bit begins to move ($\dot{\phi}_b \ge \zeta$) and cuts into the rock. Table. 1 presents the relevant mathematical expressions for all the system parameters.

Table 1. Description of Model Parameters

Symbol	Expression
τ_r	$\tau_r := c_b\left(\dot{\phi}_r - \dot{\phi}_b\right) + k_b\left(\phi_r - \phi_b\right) - c_b\dot{\phi}_b$
τ_s	$\tau_s := \mu_{sb}R_b WOB$
μ_b	$\mu_b := \mu_{cb} + (\mu_{sb} - \mu_{cb})\,\text{e}^{-\gamma_b\|\dot{\phi}_b\|/\nu_f}$

Table. 2 details all of the system parameters values taken from the experiment mentioned in Vaziri et al. (2018).

Table 2. Model Parameters, Values and Units

Symbol	Name	Value(s)/Units
μ_{cb}	Coulomb Friction Coeff.	0.0685
μ_{sb}	Static Friction Coeff.	0.0843
R_b	Bit Radius	0.0492 m
WOB	Weight-on-Bit	1760 N
γ_b	Vel. Decrease Rate	0.3
ν_f	Vel. Constant	0.1935
ζ	Small Positive Constant	10^{-6}
u	Open-Loop Top-Torque	$u \in [0, 60]$ N m
J_t	Top-Drive Inertia	13.93 kgm^2
J_b	Bit Inertia	1.1378 kgm^2
c_r	Top-Drive Damping Coeff.	11.38 N m s rad^{-1}
c_s	Torsional Damping Coeff.	0.005 N m s rad^{-1}
k_s	Torsional Stiffness Coeff.	10 N m rad^{-1}
τ_d	System-Induced Delay	0.4 s
u_h	Maximum Control Input	68.46 N m
u_l	Minimum Control Input	22.63 N m

Bifurcation diagrams (d) and (f) show that the WOB and top-torque both play an equally pivotal role for producing co-existing attractors. The region of $u = [8, 20]$ N m in (d) possesses an unstable constant drilling branch not accessible practically (or via traditional numerical integration) except with the method of numerical continuation or via some stabilising control method. As can be seen in Fig. 2(d), Stick-Slip and constant drilling attractors coexist within the region bound by $u = [21, 56]$ N m while $u = [57, 60]$ N m denotes region where the drill-string only operates in the constant drilling mode. Another important point to note is that as shown in the basins of attraction plotted in Fig. 2(e), the parameter-space defined by the range of initial conditions analysed herewith is dominated by Stick-Slip. With the adopted drill-string and bit-rock models validated via the simulation results shown in Fig. 2, this work proceeds to design and implement the Modified Integral Resonant Control with Integral Tracking aimed at eliminating the unwanted Stick-Slip oscillations featuring actuation constraints and actuation delay.

3. MODIFIED INTEGRAL RESONANT CONTROL WITH INTEGRAL TRACKING FEATURING DELAY AND CONSTRAINS

The main control objective for any effective drill-string control strategy is to minimize (ideally eliminate) the damaging Stick-Slip oscillations and guide the system into a state of constant drilling where possible (Shangxin et al., 2020). The MIRC-based damping scheme with Tracking Control is a combination of four gains with a desired reference variable viz: the Output gain λ, the Feed-Through gain κ and the Integrator gain η, which are all connected to an Integrator belonging to the MIRC; as depicted in Fig. 3(f), (MacLean and Aphale, 2020) and then a single integrator gain k_i with desired reference Ω_c. These gains are easily selected via a simple numerical search over a range of parameter-space. Two new controller states ψ and ν are defined and then embedded into equations (1) and (2) by producing extra state differential equations.
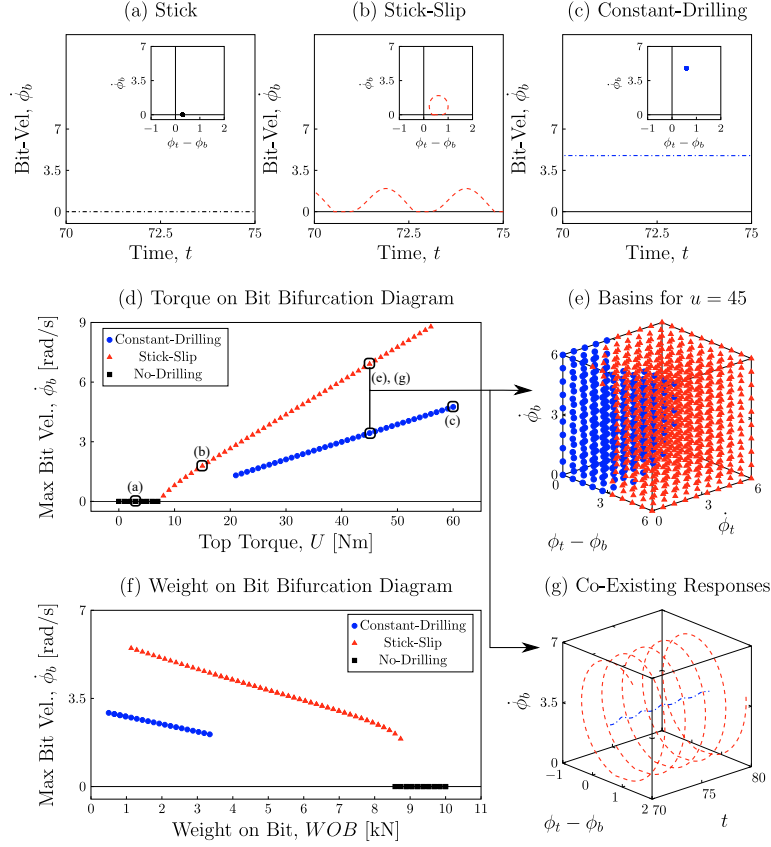
Fig. 2. Red triangles, blue circles and black squares represent the states of Stick-Slip, constant drilling and stick respectively. (a - c) represent combined time histories with phase-portraits for the top-torques of; $u = 3, 15, 60$ respectively. (d) is the central top-torque bifurcation diagram from which (a - c), (e) and (f) are generated from. (e) represents a co-existing basins plot at $u = 45$. (f) shows the Weight-On-Bit bifurcation perspective of (d). (g) shows the two co-existing responses of Stick-Slip and constant drilling together on the same phase-plane for $u = 45$.

Consequently, the system dynamics, with actuation delay, can be described by:

$$J_t \ddot{\phi}_t + (c_s + c_r) \dot{\phi}_t + k_s \phi_t - c_s \dot{\phi}_b - k_s \phi_b = u + \eta \psi_{\tau_d} + k_i \nu_{\tau_d},$$

$$J_b \ddot{\phi}_b + c_s \dot{\phi}_b + k_s \phi_b - c_s \dot{\phi}_t - k_s \phi_t = -T_b,$$

$$\dot{\psi} + \eta \kappa \psi + \lambda \left[\dot{\phi}_b - \dot{\phi}_t \right] = 0, \tag{4}$$

$$\dot{\nu} - [\Omega_d - x_1] = 0.$$

where $\psi_{\tau_d} = \psi(t - \tau_d)$ and $\nu_{\tau_d} = \nu(t - \tau_d)$ are the delayed inputs caused by the inherent delay in the top-drive. The following table details the exact scheme gains used for the following simulations seen in Fig. 3.

Table 3. Controller Parameters and Value(s)

Symbol	Name	Value(s)
u	Closed-Loop Torque Range	$u \in [u_l, u_h]$
λ	Output Feedback Gain	-10
η	Integrator Gain	70
κ	Feed-Through Gain	1
Ω_d	Desired Velocity	User Chosen
k_i	Tracking Integrator Gain	3

Fig. 3(d) shows the detailed bifurcation diagram. In this diagram, the top-torque is varied from $u \in [0, 60]$ N m.

In the experimental setup, as discussed in Table. 1, there are minimum and maximum torque constraints. To reflect this, the unstable constant-drilling solutions that are not reachable are represented by grey pentagons. When within these control input limits, the scheme is capable of finding the blue circle constant-drilling attractors and eliminating the Stick-Slip found within this region. Fig. 3(a), Fig. 3(b) and Fig. 3(c) shows the natural system response of Stick-Slip being driven to that of the other natural system response of constant drilling thanks to the scheme's resonance suppression and tracking effects. The system is first settled into a Stick-Slip regime up to $t = 30$ s and then the scheme is activated therewith. Under both actuation constraints and actuation delay, tracking a constant velocity of $\Omega_d = 2.992 \text{rad s}^{-1}$ and suppressing Stick-Slip is observed. Fig. 3(e) shows the control input graph and demonstrates a brief saturation of the upper and low control input limits and settles once constant drilling is achieved. Fig. 3(g) shows that with the scheme enabled, the initial conditions do not affect the final response of the system thereby demonstrating invariance.

4. FURTHER RESULTS

In order to verify the effectiveness of the scheme, the notion of 'Vibration Reduction Factor' (VRF) must be introduced. VRF is a relative means of comparing the
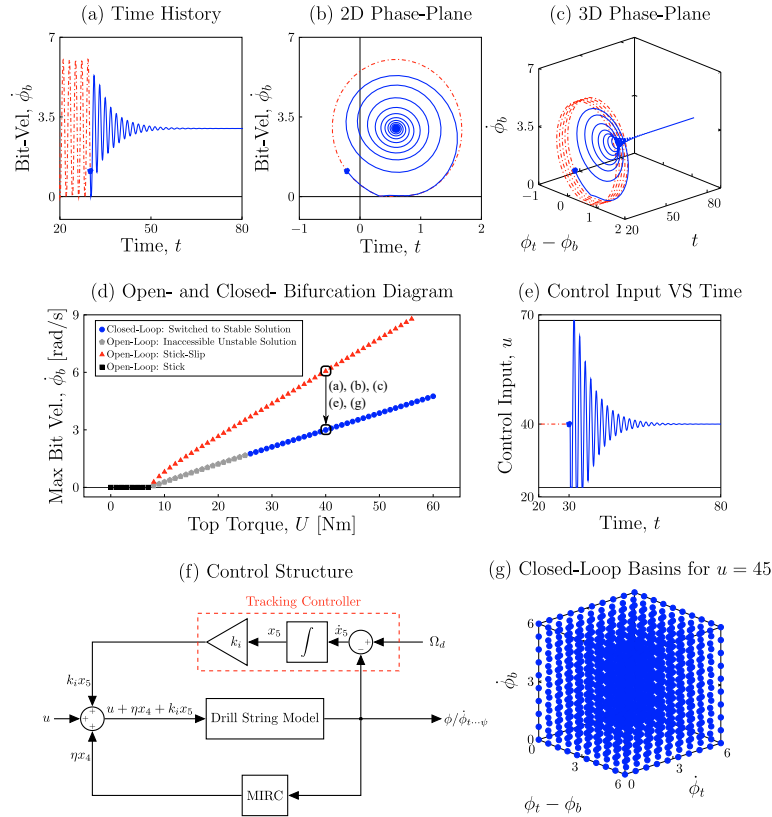
Fig. 3. (a - c) represent the time-history, 2-D and 3-D phase-plane respectively for the case in which $u = 40$. The natural system response is given by (.- red) and scheme altered response (- blue) respectively. (d) is the central top-torque bifurcation diagram from which the results of (a - c), (e) and (g) are derived and is marked to show the Stick-Slip to constant drilling transition. (e) shows the control input for this case. (f) shows the scheme's structure without delay. (g) shows the scheme controlled basins of attraction.

amplitude of a Stick-Slip oscillation in open-loop with the amplitude of the closed-loop response. There exists four possible controller outcomes, namely; case 1 ($\geq 95\%$VRF) which is constant drilling, case 2 ($\leq 95\%$VRF) and no bit-sticking which is torsional vibration, case 3 ($+ve\%$VRF) with bit-sticking (reduced Stick-Slip amplitude) and lastly, case 4 ($-ve\%$VRF) with bit-sticking (in which the Stick-Slip is made worse). Successful results lie in cases 1 and 2 respectively wherein the drill-string is no longer undergoing Stick-Slip. The formula used to classify VRF is as follows:

$$VRF\% = 100 \cdot \frac{\bar{a}_{ol} - \bar{a}_{cl}}{\bar{a}_{ol}}, \qquad (5)$$

where $\bar{a}_{ol}$ and $\bar{a}_{cl}$ are the average open-loop and closed-loop Stick-Slip amplitudes of vibration. It should be noted that this formula does not indicate if a system is under Stick-Slip or not in cases 3 and 4. In these cases, extra care is required to label and classify the response along with the VRF result. Fig. 4 shows the effects of varying the spring coefficient k_s as well as the desired velocity Ω_d. Fig. 4(c) acts as the primary bifurcation diagram for all other plots around it. In (d) the bifurcation variable is the torsional spring coefficient k_s and for each k_s, the controlled system is made to track $\Omega_d = 2.552\,\mathrm{rad\,s^{-1}}$. Fig. 4(a) and Fig. 4(e) are sub-bifurcation diagrams derived from Fig. 4(d) at $k_s = 10\,\mathrm{N\,m\,rad}$ and $k_s = 20\,\mathrm{N\,m\,rad}$ respectively in which the bifurcation parameter is the desired velocity Ω_d. Overall the scheme has great success up to $k_s = 15$ upon

which it fails to suppress Stick-Slip and guide the system to the desired velocity ($100\% VRF$) which is confirmed by Fig. 4(a). In addition to this, Fig. 4(a) shows that when $k_s \leq 15$, any desired velocity that requires a final u within the constraints mentioned, it is successful. Overall there exists some excellent robustness to the main changing system parameter k_s and the scheme, when not working optimally for $k_s > 15$, does not cause system instabilities as seen in Fig. 4(e), but overall the scheme can not stabilise the majority of velocities for this k_s range. The next simulations deal with the effects of varying actuator delay on the system to see the controller's robustness to delay in general. Tab. 4 details the simulation parameters for the effects of varying actuation delay.

Table 4. Delay Simulations Parameters

Row 1	η	λ	κ	k_i	Ω_d	τ_d
$k_s = 1$ Study	75	-10	1	5	$\in [1, 5]$	$\in [0, 2.4]$
$k_s = 10$ Study	75	-10	1	5	$\in [1, 5]$	$\in [0, 2.4]$
$k_s = 20$ Study	75	-10	1	5	$\in [1, 5]$	$\in [0, 2.4]$

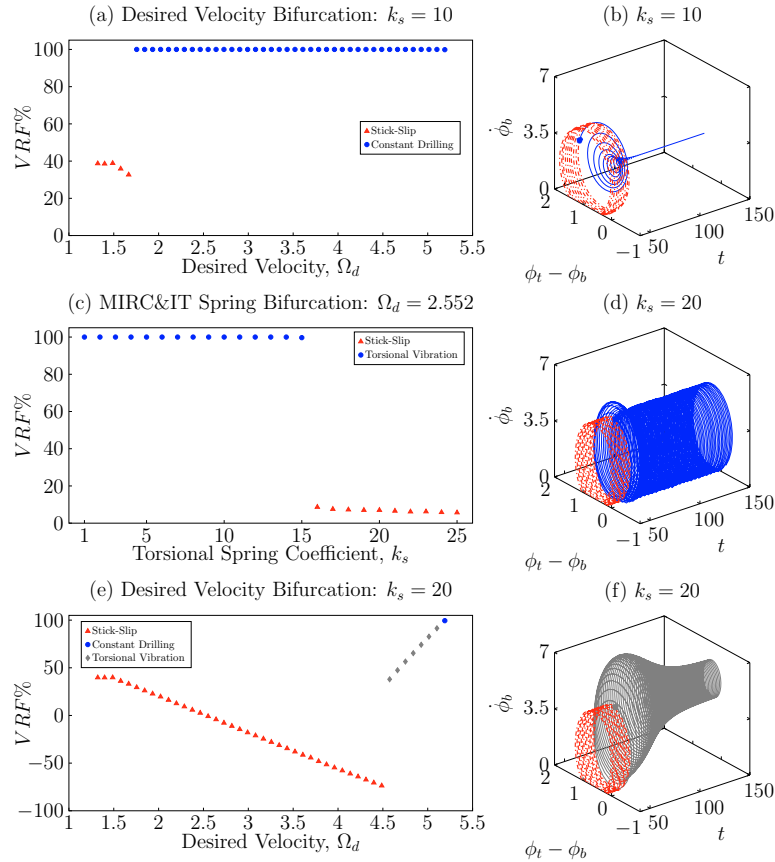| Row 2	η	λ	κ	k_i	Ω_d	τ_d [s]
$k_s = 1$ Study	75	-0.05	1	5	$\in [1, 5]$	$\in [0, 2.4]$
$k_s = 10$ Study	75	-0.05	1	5	$\in [1, 5]$	$\in [0, 2.4]$
$k_s = 20$ Study	75	-0.05	1	5	$\in [1, 5]$	$\in [0, 2.4]$

Fig. 4. (c) is the central bifurcation diagram in which the bifurcation parameter is spring coefficient k_s. Bifurcation diagrams (a) and (e) use the desired velocity Ω_d as the bifurcation parameter and are derived from (c). (b), (d) and (f) show three examples of successful, unsuccessful and partially successful responses from the bifurcation diagrams.
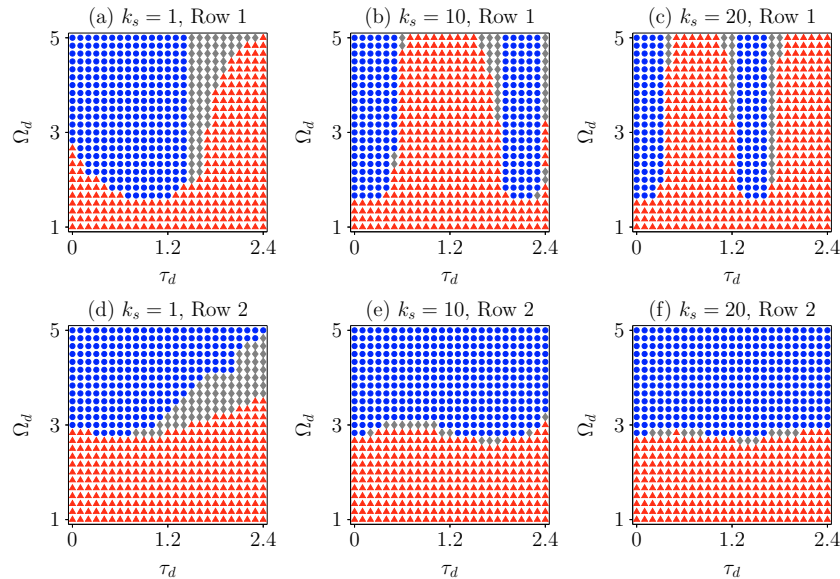

Fig. 5. (a - c) Show the effects of the row 1 gains chosen in Tab. 4 for the cases of $k_s = 1, 10, 20$ and demonstrates clear regions of success and failure in each case. (d - f) Shows the effects of the row 2 gains chosen in Tab. 4 for the cases of $k_s = 1, 10, 20$. For these cases, the change in λ creates a greater desired regime for $\Omega_d \geq 3$ for $\tau_d \in [0, 2.4]$. This comes at the price of losing access to lower desired velocities across most delays.

In Fig. 5, in the first row of simulations, there are clear regions in which the scheme successfully produces the ideal response under varying delay and even under changing k_s. In general, the higher the k_s, the harder it becomes to drive in the presence of increasing delay. In these simulations, it is shown that under the effects of varying

delay and the same actuation constraints, extra robustness to delay can be produced by altering the λ gain, but this comes at the cost of the ability to track smaller target velocities even within the actuation constraints. The overall robustness to the incredibly detrimental effect of actuator delay is an impressive feature of this scheme especially when aggressive control is not possible due to the actuation limits thereby proving its worth.

5. CLOSING REMARKS

The Modified Integral Resonant Controller (MIRC) with integral tracking demonstrates excellent stick-slip miti-gation and desired drill-bit velocity tracking capabilities, even in the presence of actuator constraints and inherent system delay. The scheme shows excellent robustness when tested for a significantly wide range of variation in the most commonly varying drill-string model parameter, namely the torsional spring coefficient. Two sub-bifurcation dia-grams, which utilise the desired velocity as the bifurca-tion parameter, confirm its success and failure in extreme cases. Consequently, a very clear and defined parameter space where the control scheme achieves constant drilling emerges. The scheme is also investigated under varying actuator delay while still under the same actuation con-straints. It is found that there exists small regions of successful constant drilling when its gains are not tuned to the system. When tuning the output feedback gain λ, it is found that greater consistent ranges of constant drilling can be produced as the cost of losing the ability to track lower desired velocities for smaller actuator delay values. Conclusively, the scheme has promising robust-ness to varying system parameters, varying actuator delay and actuation constraints; thereby proving itself to be an effective candidate for controlling such highly nonlinear systems.

REFERENCES

Bisoffi, A., Beerens, R., Heemels, W., Nijmeijer, H., van de Wouw, N., and Zaccarian, L. (2020). To stick or to slip: A reset PID control perspective on positioning systems with friction. *Annual Reviews in Control*.

Canudas-de Wit, C., Rubio, F.R., and Corchero, M.A. (2008). D-OSKIL: A new mechanism for controlling stick-slip oscillations in oil well drillstrings. *IEEE Transactions on Control Systems Technology*.

Hohl, A., Tergeist, M., Oueslati, H., Herbig, C., Ichaoui, M., Ostermeyer, G.P., and Reckmann, H. (2016). Pre-diction and mitigation of torsional vibrations in drilling systems. In *SPE/IADC Drilling Conference, Proceed-ings*.

Jardine, S., Malone, D., and Sheppard, M. (1994). Putting a damper on drilling's bad vibrations. *Oilfield Review*.

Kovalyshen, Y. (2015). Understanding root cause of stick-slip vibrations in deep drilling with drag bits. *International Journal of Non-Linear Mechanics*.

Kyllingstad, A. (2017). A comparison of stick-slip mitiga-tion tools. In *SPE/IADC Drilling Conference, Proceed-ings*.

Liu, X., Vlajic, N., Long, X., Meng, G., and Balachan-dran, B. (2014). Coupled axial-torsional dynamics in rotary drilling with state-dependent delay: stability and control. *Nonlinear Dynamics*, 78(3), 1891–1906.

MacLean, J.D. and Aphale, S.S. (2020). A Modified Linear Integral Resonant Controller for suppressing jump-phenomenon and hysteresis in micro-cantilever beam structures. *Journal of Sound and Vibration*, 480, 115365.

Navarro-López, E.M. (2009). An alternative characteriz-ation of bit-sticking phenomena in a multi-degree-of-freedom controlled drillstring. *Nonlinear Analysis: Real World Applications*.

Navarro-López, E.M. and Cortés, D. (2007). Avoiding harmful oscillations in a drillstring through dynamical analysis. *Journal of Sound and Vibration*.

Navarro-López, E.M. and Suárez, R. (2004). Practical approach to modelling and controlling stick-slip oscilla-tions in oilwell drillstrings. In *Proceedings of the IEEE International Conference on Control Applications*.

Pavone, D.R. and Desplans, J.P. (1994). Application of high sampling rate downhole measurements for analysis and cure of stick-slip in drilling. In *Proceedings - SPE Annual Technical Conference and Exhibition*.

Real, F.F., Batou, A., Ritto, T.G., Desceliers, C., and Aguiar, R.R. (2018). Hysteretic bit/rock interaction model to analyze the torsional dynamics of a drill string. *Mechanical Systems and Signal Processing*, 111, 222–233.

Ritto, T.G. and Ghandchi-Tehrani, M. (2019). Active control of stick-slip torsional vibrations in drill-strings. *JVC/Journal of Vibration and Control*.

Runia, D.J., Dwars, S., and Stulemeijer, I.P. (2013). A brief history of the shell "Soft Torque Rotary System" and some recent case studies. In *SPE/IADC Drilling Conference, Proceedings*.

Sarker, M.M., Rideout, D.G., and Butt, S.D. (2012). Ad-vantages of an lqr controller for stick-slip and bit-bounce mitigation in an oilwell drillstring. In *ASME Interna-tional Mechanical Engineering Congress and Exposition, Proceedings (IMECE)*.

Shangxin, F., Yujie, W., Guolai, Z., Yufei, Z., Shanyong, W., Ruilang, C., and Enshang, X. (2020). Estimation of optimal drilling efficiency and rock strength by using controllable drilling parameters in rotary non-percussive drilling. *Journal of Petroleum Science and Engineering*, 193, 107376.

Vaziri, V., Kapitaniak, M., and Wiercigroch, M. (2018). Suppression of drill-string stick-slip vibration by sliding mode control: Numerical and experimental studies. *Eu-ropean Journal of Applied Mathematics*.

Vromen, T., Dai, C.H., Van De Wouw, N., Oomen, T., Astrid, P., and Nijmeijer, H. (2015). Robust output-feedback control to eliminate stick-slip oscillations in drill-string systems. In *IFAC-PapersOnLine*.

Vromen, T., Detournay, E., Nijmeijer, H., and Van De Wouw, N. (2019). Dynamics of drilling systems with an antistall tool: Effect on rate of penetration and mechanical specific energy. *SPE Journal*.